Signal Processing 207 (2023) 108960

Contents lists available at ScienceDirect

Signal Processing

journal homepage: www.elsevier.com/locate/sigpro

A polynomial multiple variance method for impulse response measurement☆

Alberto Carini[a,*], Riccardo Forti[b], Simone Orcioni[c]

[a] DIA, University of Trieste, Trieste 34127, Italy
[b] SMH Technologies, Pordenone 33089, Italy
[c] DII, Università Politecnica delle Marche, Ancona 60131, Italy

ARTICLE INFO

Article history:
Received 19 October 2022
Revised 23 December 2022
Accepted 2 February 2023
Available online 5 February 2023

Keywords:
Multiple variance method
Volterra filter
Impulse response measurement

ABSTRACT

This manuscript describes a methodology for measuring the first-order Volterra kernel of a discrete-time nonlinear system, that is, the impulse response for small signal amplitudes of the nonlinear system. In the proposed approach, multiple linear identifications are performed using the same excitation signal multiplied by different gains, and the first-order Volterra kernel is obtained from a polynomial interpolation of the measured values. Any linear identification method proposed in the literature can be used with this approach. The proposed approach is a multiple variance (MV) method that, in contrast to all other MV methods, aims to estimate one of the kernels of the Volterra model, the first-order kernel, with high precision. The manuscript discusses the proposed methodology, determines the mean square deviation (MSD) due to noise of the measured coefficients, and the value of the optimal gains that minimize the MSD. Remarkably, it is shown in the manuscript that the optimal gains assume only a reduced set of values that depends on the order of nonlinearity. The optimal number of measurements is also determined. The conditions under which the proposed methodology is more convenient than the classical linear methods are discussed. The experimental results demonstrate the proposed methodology and its strengths.

1. Introduction

Impulse response measurement is a transverse tool used in many fields of technology [1–14]. The impulse response fully characterizes any linear time-invariant system. Often, nonlinearities affect the measurement of the impulse response. These nonlinearities could be intrinsic to the system under measurement, which could be mildly nonlinear rather than linear, or could be generated by the measurement system itself when taken to its limit. For example, in the measurement of the room impulse response, nonlinearities have been observed at high reproduction volumes, caused by the saturation of the power amplifier or by nonlinearities arising in the loudspeaker. In electrodynamic loudspeakers, nonlinearities can arise because of the nonlinear stiffness of the suspensions or nonuniform magnetic fields [15]. In the presence of nonlinearities, the impulse response depends on the amplitude of the input signal [16,17]. Engineers and technicians want to determine the impulse response for low signal amplitudes, which is the first-order kernel of the Volterra expansion of the system. Most impulse response measurement methods proposed in the literature consider the measurement of linear systems and ignore nonlinearities [18–29]. Therefore, they are affected by the nonlinearity of the measurement system. Motivated by this problem, we propose a novel method for the measurement of impulse response that is robust towards nonlinearities.

One of the early approaches to impulse response measurement directly applied the definition of impulse response and measured the system by applying a pulse signal. In acoustics, gunshots, balloon explosions, and clappers have been used to directly record impulse responses. The same approach was used by generating a pulse using electronic means [18]. To contrast the effect of noise, the response to periodic pulse excitation signals can be averaged. The repetition period should be sufficiently large to avoid aliasing errors. In the presence of additive Gaussian noise, the signal-to-noise ratio (SNR) improves by 3 dB each time the number of averaged periods doubles. The main limitation of a pulse excitation

☆ The following co-authors are members of EURASIP: Alberto Carini and Simone Orcioni. Riccardo Forti was with DIA - University of Trieste when he participated in this research. He is now with SMH Technologies.

* Corresponding author.
E-mail addresses: acarini@units.it (A. Carini), s.orcioni@univpm.it (S. Orcioni).

https://doi.org/10.1016/j.sigpro.2023.108960

signal is its low power. The maximum amplitude of the pulse is often limited by the measurement system, which can saturate high-amplitude pulses or can even be damaged by them.

One of the most successful approaches for impulse response measurement was proposed by Schroeder, and is based on the use of maximal length sequence (MLS) excitation [19]. An MLS is a binary pseudo-noise periodic sequence with period $2^n - 1$ and $n \in \mathbb{N}$ [30]. MLSs have a white broadband spectrum and almost perfect autocorrelation, that is, a periodic pulse train apart from a small offset, which is negligible for large periods. With MLSs, the impulse response is identified using the cross-correlation method by cross-correlating the measured output with the MLS input. Noise rejection can be improved by averaging the different periods of MLS. In the presence of nonlinearities, MLSs generate visible distortion artifacts, often in the form of spikes that overlap with the measured impulse response [31]. In reality, these spikes are scaled replicas of the same impulse responses. In fact, they originate from the following property of the MLS: the product of an MLS $m(n)$ with a delayed version of the same MLS $m(n-i)$ is again the same MLS delayed by a different quantity $m(n-j)$ [32]. To contrast in part the effect of nonlinearities, inverse repeated MLSs (IRMLSs) have been proposed and are obtained by inverting the sign of any odd-index sample in an MLS [33]. It has been proven in the literature that IRMLSs are immune to even order nonlinearities [20]. Other sequences similar to MLSs are the perfect periodic sequences (PPSs) used for linear system identification [21,34,35]. A PPS for a linear system is a periodic sequence with perfect autocorrelation, that is, a periodic pulse train. Thus, by using a PPS input signal, the impulse response can be measured with the cross-correlation approach. The PPSs for linear system identification have no specific protection against nonlinearities. Moreover, PPSs are not binary sequences like MLSs; however, ternary PPSs have been proposed in the literature [36–38]. Odd-perfect sequences (ODD-PSEQs) have also been proposed [22]. They are symmetrical, quasi-binary sequences, and except for a leading zero, all samples assume only two values $\{+1, -1\}$. Moreover, their period is formed by two semi-periods, one the opposite of the other, and thus they allow identification of the impulse response immune to even order nonlinearities as the IRMLSs.

Currently, the most successful technique for impulse response measurement is based on exponential sweep excitation. This technique has been developed almost simultaneously by different researchers [39,40] and was later improved by introducing the synchronized swept technique [41]. Measurements with exponential sweeps are appreciated for their robustness to nonlinearities. It was shown in Farina [39] that if the measurement system can be modeled as a Hammerstein filter, that is, a memoryless nonlinearity followed by a linear filter, the artifacts originating from the nonlinear terms can be segregated at negative times and windowed out. In reality, it was recently shown that the nonlinear kernels of the Hammerstein filter still affect the measures with exponential sweeps of Farina [39], Müller and Massarani [40], Novak et al. [41] unless the measurement is corrected using the information of higher-order kernels [42]. Moreover, nonlinearities are rarely memoryless, and research has shown that nonlinearities with memory also alter measurements with exponential sweeps [43,44].

Many other measurement methods have been proposed for the impulse response measurement of linear systems without taking any particular measure to prevent the effect of nonlinearities. It is worth mentioning: i) the time-stretched pulse techniques [23,24], using a pulse expanded in time; ii) the measurements based on Golay codes [25], where the system is measured twice using sequences taken among the Golay codes; iii) the time delay spectroscopy [26,27] that uses a linear sweep excitation; iv) the stepped sine technique, where the excitation signal is composed of pure tones whose frequency increases in steps [28]; v) the perfect periodic sweeps [29], which are perfect periodic sequences constructed in the frequency domain with an ideally flat magnitude response and linear group delay.

More recently, different techniques have been proposed for the robust measurement of impulse response in the presence of nonlinearities. These techniques directly model the measurement system as a nonlinear filter, and attempt to estimate its linear component. A first approach was proposed in Carini et al. [45], Carini et al. [46,47,48], where the measurement system was modeled as a Legendre nonlinear (LN) filter [45,46] or a Wiener nonlinear (WN) filter [45,46]. The LN and WN filters are orthogonal polynomial filters. Their basis functions are orthogonal for a certain distribution of input samples (uniform for the LN filters and Gaussian for the WN filters). It was shown that orthogonal polynomial filters admit PPSs, which in this context are periodic sequences that guarantee perfect orthogonality of the basis functions over a period [49]. Using a PPS for LN or WN filters, it is possible to measure the linear part of the system under measurement, that is, the first-order kernel, while simultaneously removing the influence of other nonlinear kernels. Later in Carini et al. [50], orthogonal periodic sequences (OPSs) were introduced and applied to the robust measurement of impulse response in the presence of nonlinearities [51,52]. The OPSs allow estimating a broad class of nonlinear filters, the functional link polynomial (FLiP) filters, which include many popular nonlinear filters, including well-known Volterra filters. Given a persistently exciting periodic input sequence, an OPS is a periodic sequence that allows estimating one of the diagonals of the FLiP filter using the cross-correlation method. In impulse response measurements, the OPS is used to estimate the first-order kernel of the Volterra filter. Compared to PPSs, OPSs can be more easily developed, and for the same input sequence, OPSs suitable for identifying different nonlinear filters can be obtained. However, OPSs are more sensitive to noise than PPSs.

This study proposes a novel approach for the measurement of the first-order Volterra kernel, that is, the impulse response for low amplitudes of a nonlinear system. This approach is based on the use of classical methodologies applied to measure the impulse response of linear systems; however, the excitation signal is now applied multiple times with different gains. Any linear impulse response measurement method can be applied; for example, any of the previously mentioned methods [18–29,39–41]. The first-order kernel is extracted using polynomial interpolation from multiple measurements performed with different gains.

The approach proposed in this paper was briefly introduced in a conference paper [53]. The theory has been improved by directly exploiting the symmetric distribution of gains, as explained in Section 3. The manuscript determines the expression of the mean square deviation (MSD) of the measured impulse response samples for additive Gaussian noise. The optimal value of the gains that minimize the MSD is also found. It is shown that even when considering a large number of measurements, the optimal gains assume only a reduced number of values, which depends on the order of nonlinearity. Moreover, the optimal number of measurements is obtained. The optimal values of the gains and number of measurements are reported in tables to facilitate their applicability in common practice. This paper also discusses when the proposed method is convenient with respect to multiple measurements performed at low input powers to avoid the effect of nonlinearities.

The proposed approach belongs to the class of multiple variance methods, in which the input signal is applied multiple times with different variances, that is, powers. Multiple variance techniques have already been proposed in the literature [54], but for purposes different from those presented in this paper [55]. The approach in Orcioni [54] used multiple variances to contrast the lo-

cality of identification when a Wiener model was identified using the Lee–Schetzen method. With a single input variance, the model represents well the behavior of the nonlinear system only for input powers that are close to the chosen value. To expand the validity of the Wiener model, in Orcioni [54], different kernels were estimated with different input signal variances, thereby minimizing the mean-square error between the output of the system and that of the model. In contrast, in this study, the multiple variance approach is used to estimate with high accuracy a single kernel of the nonlinear model, the first-order kernel, and polynomial interpolation is used for this purpose.

The main original contributions of the manuscript are the following:

- This study discusses a novel multiple-variance approach for impulse response measurements in the presence of nonlinearities.
- This approach determines the impulse response for small signals, that is, the first-order Volterra kernel of the system under measurement.
- This method is based on classical linear techniques with an excitation signal applied multiple times with different gains.
- Any classical linear identification technique can be used in combination with the proposed approach.
- The MSD of the measured first-order Volterra kernel was determined and used to determine the optimal values of the gains and number of measurements.
- It was shown that the optimal values of the gains assume a reduced number of values, which depends only on the order of the measured nonlinear system.
- The optimal values of gain and number of measurements are reported in tables to facilitate their applicability in common practice.
- It is discussed when the proposed approach is convenient with respect to multiple measurements performed at a low excitation power to avoid nonlinearities.

In contrast to other approaches for the robust measurement of the impulse response in the presence of nonlinearities, for example, Carini et al. [45], Carini et al. [46,47,48,51,52], the proposed approach requires only mild knowledge of the order of nonlinearity of the system, and applies classical linear techniques for the measurement. Thus, it is immediately applicable to current instrumentation because only the input gain has to be changed. The main drawback is the requirement to perform the measurement multiple times to extract the impulse response for low signal amplitudes.

Recent applications involving nonlinear systems that could benefit from the proposed approach can be found in Forti et al. [53], Roinila and Messo [56], Kannan and Meyer [57], Von Hauff [58], Ciucci [59], Altan and Hacıoğlu [60], Tamilselvi et al. [61], Meddings et al. [62], Gharbi et al. [63], Chen et al. [64].

The remainder of this paper is organized as follows. Section 2 briefly reviews the theory of Volterra filters. Section 3 presents the proposed method and computes the MSD of the measured samples for additive Gaussian noise. Section 4 derives the optimal value of the gains and number of measurements. Section 5 discusses when the proposed method is convenient with respect to a classical linear identification performed at a low input power to avoid nonlinearities. Section 6 presents the experimental results of the measurement of the first-order kernel of a real device under various nonlinear conditions. Section 7 provides concluding remarks.

The following notation is used throughout the paper: calligraphic letters denote operators, $E[\cdot]$ is the expectation, $\lceil\cdot\rceil$ is the first integer greater than the argument, bold lowercase letters denote arrays, and bold uppercase letters denote matrices.

2. Volterra filters

Volterra filters are polynomial filters derived from double truncation with respect to the order and memory of the Volterra series [17]. According to the Stone-Weierstrass theorem, they can arbitrarily well approximate any causal, discrete-time, time-invariant, finite-memory, continuous nonlinear system, whose input-output relationship can be expressed by a nonlinear function f of the last input samples:

$$y(n) = f[x(n), x(n-1), \ldots, x(n-N+1)], \tag{1}$$

where $x(n)$ is the nth sample of the input signal x and belongs to a compact in $\mathbb{R}$, $y(n)$ is the nth sample of the output signal y, and N is the filter memory length.

A Volterra filter of order K and memory N has input-output relationship

$$y(n) = \sum_{k=0}^{K} \mathcal{H}_k(x)(n), \tag{2}$$

where $\mathcal{H}_k(x)$ is a homogeneous polynomial operator of order k and memory N applied to the input signal x and $\mathcal{H}_k(x)(n)$ is its nth sample. Accordingly, $\mathcal{H}_0(x)(n)$ for all n is a constant $h_0 \in \mathbb{R}$. $\mathcal{H}_1(x)$ is a linear operator written as

$$\mathcal{H}_1(x)(n) = \sum_{i=0}^{N-1} h_{1,i} x(n-i), \tag{3}$$

where $h_{1,i}$ are the coefficients of the first-order Volterra kernel, also known as the linear kernel. $\mathcal{H}_2(x)$ is a quadratic operator that in the triangular form is [17]

$$\mathcal{H}_2(x)(n) = \sum_{i_1=0}^{N-1} \sum_{i_2=i_1}^{N-1} h_{2,i_1,i_2} x(n-i_1) x(n-i_2), \tag{4}$$

where h_{2,i_1,i_2} are coefficients of the second-order Volterra kernel. In general, the kth order operator $\mathcal{H}_k(x)$ has the triangular form:

$$\mathcal{H}_k(x)(n) = \sum_{i_1=0}^{N-1} \sum_{i_2=i_1}^{N-1} \cdots \sum_{i_k=i_{k-1}}^{N-1} h_{k,i_1,\ldots,i_k} x(n-i_1) \cdot \ldots \cdot x(n-i_k), \tag{5}$$

where $h_{k,i_1,\ldots,i_k}$ are the coefficients of the kth order Volterra kernel.

The method discussed in the next section relies on the homogeneity property of operator $\mathcal{H}_k(x)$. If the input is multiplied by factor A, then

$$\mathcal{H}_k(Ax) = A^k \mathcal{H}_k(x). \tag{6}$$

Moreover, we exploit the fact that the odd order homogeneous operators are odd, and the even order ones are even, that is,

$$\mathcal{H}_{2k}(-x) = \mathcal{H}_{2k}(x), \tag{7}$$

$$\mathcal{H}_{2k+1}(-x) = -\mathcal{H}_{2k+1}(x). \tag{8}$$

3. The polynomial multiple variance method

In this Section, we first introduce the proposed method and then study the influence of noise on measurements.

3.1. The proposed method

Assume that we are coping with a nonlinear system that can be modeled as a Volterra filter of order K, memory N, plus noise:

$$y = \mathcal{H}(x) + v = \sum_{k=0}^{K} \mathcal{H}_k(x) + v, \tag{9}$$

where $\mathcal{H}$ is the Volterra operator defined by (2), v is an output additive noise signal, and the time notation (n) has been dropped for compactness. We want to measure the coefficients of the linear kernel $h_{1,i}$ for $i = 0, \ldots, N-1$, which correspond to the system impulse response samples for small signals (when the constant term h_0 is neglected).

Let us consider any of the linear identification approaches proposed in the literature. Each of these approaches defines a linear operator $\mathcal{L}_i$ from the space of sequences to $\mathbb{R}$, such that for the specific input sequence x and linear output sequence $y = \mathcal{H}_1(x)$,

$$\mathcal{L}_i[\mathcal{H}_1(x)] = h_{1,i}. \tag{10}$$

Examples of the linear operator $\mathcal{L}_i$ are reported in Appendix A.

For compactness, in what follows $\mathcal{L}_i[\mathcal{H}_1(x)]$ is simply denoted as $\mathcal{L}_i\mathcal{H}_1(x)$ exploiting the concatenation of the operators.

Since $\mathcal{L}_i$ is linear, when the operator is applied to (9),

$$\mathcal{L}_i(y) = \mathcal{L}_i\mathcal{H}(x) + \mathcal{L}_i(v) = \sum_{k=0}^{K} \mathcal{L}_i\mathcal{H}_k(x) + \mathcal{L}_i(v). \tag{11}$$

and in the considered conditions (11) does not equal to $h_{1,i}$ both for the presence of the noise v and of the nonlinear terms $\mathcal{H}_k(x)$, for $k \neq 1$.

In the following, a multiple variance methodology is adopted to measure $h_{1,i}$: the input signal x is applied multiple times, multiplied by different factors A_m, and the corresponding output signals y_m are used to estimate $h_{1,i}$. For the homogeneity property in (6), when x is multiplied by A_m, the output y_m becomes

$$y_m = \mathcal{H}(A_m x) + v_m = \sum_{k=0}^{K} A_m^k \mathcal{H}_k(x) + v_m, \tag{12}$$

where v_m is the additive output noise of y_m. By applying the linear operator $\mathcal{L}_i$ to Eq. (12), we obtain

$$\mathcal{L}_i(y_m) = \sum_{k=0}^{K} A_m^k \mathcal{L}_i\mathcal{H}_k(x) + \mathcal{L}_i(v_m), \tag{13}$$

which, apart from the noise term, is a polynomial in A_m with the coefficients $\mathcal{L}_i\mathcal{H}_k(x)$. For a sufficiently large number of gains A_m, it is possible to estimate the terms $\mathcal{L}_i\mathcal{H}_k(x)$ for $k = 0, \ldots, K$, with polynomial fitting, and thus obtain a measure of $h_{1,i}$ from the estimate of $\mathcal{L}_i\mathcal{H}_1(x)$.

Different strategies can be followed to choose the gains A_m: they can be asymmetrically or symmetrically distributed around zero. The symmetric distribution has many advantages: it minimizes the condition number of the Vandermonde matrix of the nodes involved in polynomial fitting [65,66]. It also allows us to simplify the estimation problem by eliminating all even-order nonlinear terms, as shown shortly. Thus, in the following, we assume that the input signal x is applied $2M$ times with gains A_m, $-A_m$ for $m = 1, \ldots, M$.

Since $\mathcal{H}_k(x)$ is odd for k odd and even for k even, when x is multiplied by $-A_m$, the system output y_{-m} is:

$$y_{-m} = \mathcal{H}(-A_m x) + v_m = \sum_{k=0}^{K} (-1)^k A_m^k \mathcal{H}_k(x) + v_m. \tag{14}$$

The estimation of $h_{1,i}$ can be simplified by forming the terms

$$d_m = \frac{\mathcal{L}_i(y_m) - \mathcal{L}_i(y_{-m})}{2} = \\ = \sum_{r=1}^{\lceil K/2 \rceil} A_m^{2r-1} \mathcal{L}_i\mathcal{H}_{2r-1}(x) + \frac{\mathcal{L}_i(v_m) - \mathcal{L}_i(v_{-m})}{2} \tag{15}$$

for $m = 1, \ldots, M$ and by exploiting the cancellation of even-order terms. Note that for K even, the polynomial fitting of (13) requires at least $K+1$ measures with different gains A_m, because we have $K+1$ coefficients to fit. On the contrary, the polynomial fitting of (15) can be performed with only K measures, since we have $\lceil K/2 \rceil$ coefficients to fit and we need two measures for each term d_m.

Define the $M \times 1$ vectors

$$\boldsymbol{d} = [d_1, d_2, \ldots, d_M]^T, \tag{16}$$

$$\boldsymbol{v} = [\frac{\mathcal{L}_i(v_1) - \mathcal{L}_i(v_{-1})}{2}, \frac{\mathcal{L}_i(v_2) - \mathcal{L}_i(v_{-2})}{2}, \ldots, \\ \frac{\mathcal{L}_i(v_M) - \mathcal{L}_i(v_{-M})}{2}]^T, \tag{17}$$

the $\lceil K/2 \rceil \times 1$ vector

$$\boldsymbol{h} = [\mathcal{L}_i\mathcal{H}_1(x), \mathcal{L}_i\mathcal{H}_3(x), \ldots, \mathcal{L}_i\mathcal{H}_R(x)]^T, \tag{18}$$

with $R = 2\lceil K/2 \rceil - 1$, and the $\lceil K/2 \rceil \times M$ Vandermonde-like matrix

$$\boldsymbol{A} = \begin{bmatrix} 1 & 1 & \ldots & 1 \\ A_1 & A_2 & \ldots & A_M \\ A_1^3 & A_2^3 & \ldots & A_M^3 \\ \vdots & & & \vdots \\ A_1^R & A_2^R & \ldots & A_M^R \end{bmatrix}. \tag{19}$$

Writing (15) for $m = 1, \ldots, M$ in matrix form results in

$$\boldsymbol{d} = \boldsymbol{A}^T \boldsymbol{h} + \boldsymbol{v}. \tag{20}$$

Provided $M \geq \lceil K/2 \rceil$ and $\boldsymbol{A}\boldsymbol{A}^T$ is invertible,

$$\boldsymbol{h} = (\boldsymbol{A}\boldsymbol{A}^T)^{-1}\boldsymbol{A}\boldsymbol{d} - (\boldsymbol{A}\boldsymbol{A}^T)^{-1}\boldsymbol{A}\boldsymbol{v}. \tag{21}$$

Remark 1. Neglecting the noise effect, $\boldsymbol{h}$ can be estimated with

$$\widehat{\boldsymbol{h}} = (\boldsymbol{A}\boldsymbol{A}^T)^{-1}\boldsymbol{A}\boldsymbol{d}, \tag{22}$$

and thus $h_{1,i}$ can be evaluated as

$$\widehat{h}_{1,i} = \boldsymbol{e}_1^T \boldsymbol{h} = \boldsymbol{e}_1^T (\boldsymbol{A}\boldsymbol{A}^T)^{-1}\boldsymbol{A}\boldsymbol{d}, \tag{23}$$

with $\boldsymbol{e}_1$ the first column of the $\lceil K/2 \rceil \times \lceil K/2 \rceil$ identity matrix.

3.2. The effect of noise on the measurement

Provided the nonlinear system has an order lower than or equal to K, comparing Eq. (21) with (22) it can be observed that in noise absence, i.e., for $\boldsymbol{v} = 0$, the measure in (23) perfectly estimate $h_{1,i}$. On the contrary, when $\boldsymbol{v} \neq 0$ the measure is affected by an error,

$$\epsilon_i = \widehat{h}_{1,i} - h_{1,i} = \boldsymbol{e}_1^T (\boldsymbol{A}\boldsymbol{A}^T)^{-1}\boldsymbol{A}\boldsymbol{v}, \tag{24}$$

and the mean square deviation (MSD) of the estimated coefficient is

$$\text{MSD} = E\big[(\widehat{h}_{1,i} - h_{1,i})^T (\widehat{h}_{1,i} - h_{1,i})\big] \\ = \boldsymbol{e}_1^T (\boldsymbol{A}\boldsymbol{A}^T)^{-1}\boldsymbol{A} E[\boldsymbol{v}\boldsymbol{v}^T]\boldsymbol{A}^T (\boldsymbol{A}\boldsymbol{A}^T)^{-1}\boldsymbol{e}_1. \tag{25}$$

Remark 2. In the hypothesis that the noise terms $\mathcal{L}_i(v_l)$, for $l = \pm 1, \ldots, \pm M$, are uncorrelated with each other and are Gaussian distributed with zero mean and variance σ_v^2, the MSD simplifies to

$$\text{MSD} = \frac{1}{2}\boldsymbol{e}_1^T (\boldsymbol{A}\boldsymbol{A}^T)^{-1}\boldsymbol{e}_1 \sigma_v^2. \tag{26}$$

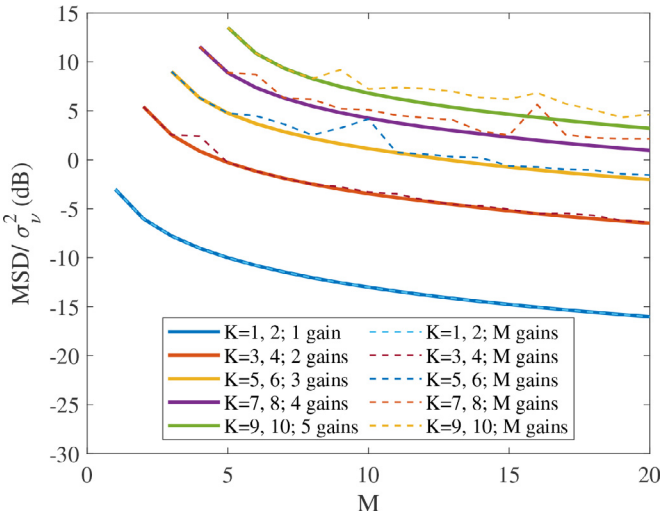

Fig. 1. Optimal value of MSD/σ_v^2 vs. M for $\lceil K/2 \rceil$ different A_m values (continuous lines) and for M different A_m values (dashed lines).

4. The optimal gains

It is clear from (19) to (26) that the choice of gains A_m influences the resulting MSD, and that there must exist an optimal choice of gains that minimize it.

Given the order K of the nonlinear model, the number M of positive gains, and the maximum gain conventionally set to 1, the optimal gains A_m are those that minimize the nonlinear function

$$J(A_1, \ldots, A_M) = \frac{\text{MSD}}{\sigma_v^2} = \frac{1}{2} \boldsymbol{e}_1^T (\boldsymbol{A}\boldsymbol{A}^T)^{-1} \boldsymbol{e}_1, \tag{27}$$

subject to $0 < A_m \leq 1$ for $m = 1, \ldots, M-1$ and $A_M = 1$. Note that the same function is obtained for both $K = 2k+1$ and $K = 2k+2$, with $k \in \mathbb{N}$, and thus, the same set of gains is optimal for two consecutive orders: odd and even. Any tool for the minimization of multiple variable nonlinear functions can be used to minimize J. For example, in MATLAB® the `fminsearch` and `fmincon` functions can be used for this purpose. From our initial experiments on the minimization of (27), it appeared immediately clear that the optimal gains tend to cluster around a limited number of values. To reduce the number of different gains, in Forti et al. [53], the optimal values of A_m were quantized before their use in identification. Later, we realized that the positive optimal gains cluster around exactly $\lceil K/2 \rceil$ values. Moreover, we observed that if, in the minimization of (27), we impose that the M gains A_m assume at most $\lceil K/2 \rceil$ different values, the optimal J is always equal to or lower than the value obtained considering M different gains.

As a matter of fact, Fig. 1 shows the minimum value of the cost function in (27) for different orders K versus the number of positive gains M both in case of $\lceil K/2 \rceil$ gains and of M different gains. Note that the curves for M different gains were obtained by performing, for each K and M, 10,000 runs of the optimization algorithm starting from a random initialization of the gains in the interval $[0, 1]$ and selecting the minimum value. Clearly, for low K and M, the continuous and dashed curves coincide. In contrast, for large K and M, the optimization with M different values is always suboptimal.

Remark 3. The results of Fig. 1 indicate that $\lceil K/2 \rceil$ gains are sufficient to optimize (27).

Clearly, when $M > \lceil K/2 \rceil$ some gain will be used multiple times, i.e., multiple measurements shall be performed with the same gain.

Fig. 2 shows the optimal value of the gains for different orders K from 3 to 10 and for M ranging from 1 to 50 (for $K = 1$ or 2, we have only one value for the gain and $A_m = 1$ for all m). The asterisk indicates that the gain has been selected multiple times and the circle only one time. The repetitions favor the lowest gains, as expected, because the measurements at the lowest gains are the most affected by noise. The continuous curves in Fig. 1 and the optimal gains in Fig. 2 were obtained by optimizing (27) for any possible combination of repeated gains and selecting the optimal solution.

Remark 4. For large M, the continuous curves in Fig. 1 decrease by 3 dB for any doubling of M, i.e., the MSD reduces by 3 dB for any doubling of the data.

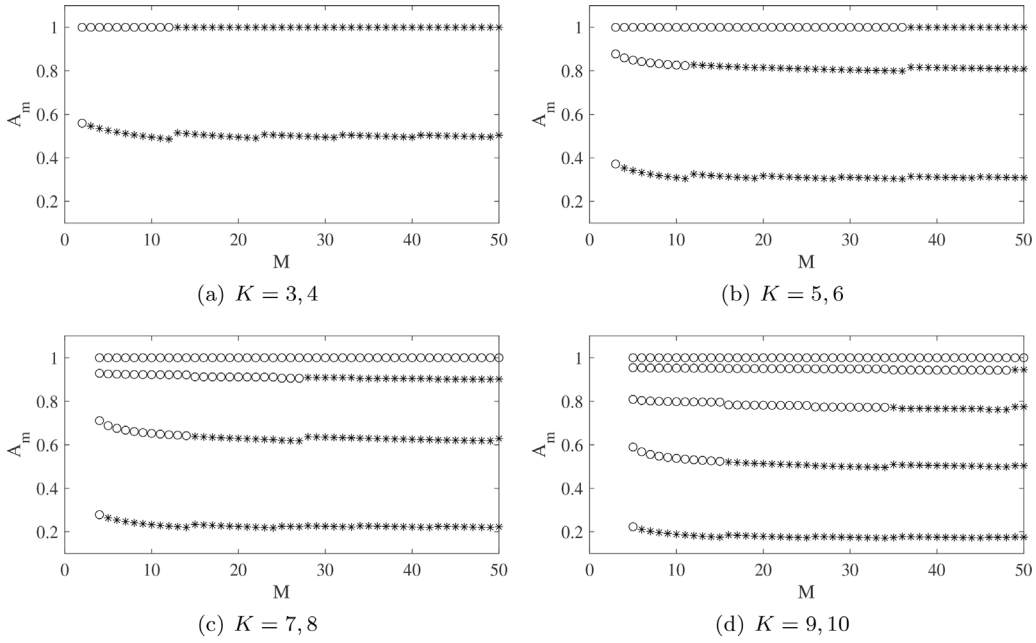

Fig. 2. Positive optimal gains A_m vs. M for different order K. The asterisk indicates the gain has been selected multiple times, the circle only one time.

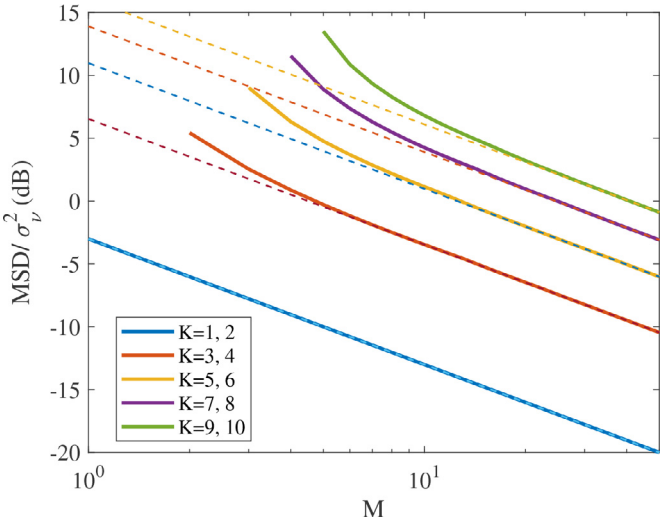

Fig. 3. Optimal value of MSD/σ_ν^2 vs. M for $\lceil K/2 \rceil$ different A_m values (continuous lines) and 3 dB slope support curves (dashed lines).

This is the same MSD reduction achieved by doubling the period of the MLS, the PPS, or the length of the exponential sweep. This property can be better appreciated from Fig. 3, where a logarithmic scale was used on the X-axis, and M ranges from 1 to 50. The dashed lines are the 3 dB slope support lines, and they overlap with the continuous curves for large M. This property inspires the following criterion for the optimal choice of M:

For each K choose the value of M that reaches the 3 dB slope line apart from a dB fraction.

The reason for this rule is that we can achieve the same MSD improvement obtained by increasing M beyond this value, by simply increasing the period or length of the sequence used in the identification.

Remark 5. Table 1 provides for each K the optimal value of M according to this rule and the corresponding optimal positive gains A_m with their multiplicity for a 1 dB difference from the 3 dB slope line. Table 2 provides the same information for a 0.5 dB difference.

5. Discussion

A natural question is when the proposed PMV method is more convenient than classical linear methods. An intuitive answer is that this depends on the level of nonlinearity. If the system under measurement, even at the highest input amplitude, has a very mild nonlinearity, so mild that its effect on the measurement with the operator $\mathcal{L}_i$ is negligible in comparison to the noise effect, the proposed approach would not be necessary. In contrast, for stronger nonlinearities, we must expect the method to perform better than standard approaches. The effect of the nonlinearity depends on the amplitude of the input signal. According to (13), by reducing the amplitude of the input signal x by a factor A_m, the influence of the nonlinear terms $\mathcal{H}_k(x)$ for $k = 2, \ldots, K$ is reduced by at least a factor A_m^2. Thus, another possible way to measure the impulse response is to scale x by a factor A sufficiently small to neglect the effect of nonlinearities and average the results of multiple measurements to compensate for the reduced SNR ratio. For the same amount of data, that is, measurements, we determine in the following when the PMV method should be preferred over multiple averaged measurements at a single low amplitude A. For this purpose, we compare the MSD of the two methods. The MSD of the PMV method is reported in (26) and is indicated by MSD_{PMV} in this section. It is shown in Appendix B that by averaging $2M$ measurements performed with the operator $\mathcal{L}_i$ and a sufficiently low amplitude input signal Ax, the MSD is

$$\text{MSD}_{\text{Av}} = \frac{\sigma_\nu^2}{2MA^2}, \tag{28}$$

where σ_ν^2 is the variance of the noise terms $\mathcal{L}_i(\nu_m)$.

According to (26) and (28), $\text{MSD}_{\text{PMV}} \leq \text{MSD}_{\text{Av}}$ for all A satisfying the following inequality,

$$A \leq \hat{A} = \sqrt{\frac{1}{M\boldsymbol{e}_1^T(\boldsymbol{A}\boldsymbol{A}^T)^{-1}\boldsymbol{e}_1}}. \tag{29}$$

According to (29), the PMV method should be preferred whenever the input signal has to be scaled by a factor lower than $\hat{A}$ to neglect the effect of nonlinearities.

Remark 6. Table 3 provides the value of $\hat{A}$ for the optimal values of M and gains A_m of Tables 1 and 2. For orders $K \leq 6$, i.e., for the most commonly used orders, $\hat{A}$ presents large values and the PMV method is often advantageous even for very mild nonlinearities.

Measuring the first-order Volterra kernel using the proposed approach requires some initial choice. First, we must choose a linear impulse response measurement method: any classical approach can be applied. Then, the impulse response length must be determined. This is typically achieved through trial-and-error procedure or by exploiting the experience of the researcher/technician performing the measurement. An important choice is the order of nonlinearity we assume to cope with. To determine the order of nonlinearity, the authors suggest performing harmonic analysis at the maximum planned input power. The highest relevant harmonic determines the order of nonlinearity K. Chosen K, the number of measurements to be performed and the input gain to be used in each measurement are reported in Tables 1 and 2. The gains are normalized and gain 1.0 corresponds to the maximum input power considered. The next section presentes some experimental results following these guidelines.

6. Experimental results

We consider the identification of a real nonlinear device, that is, a Behringer MIC100 vacuum tube preamplifier. Acting on the gain potentiometer of the preamplifier, it is possible to create different nonlinear scenarios characterized by different distortion levels. In the experiment, 17 different settings of the gain potentiometer were considered, and they are indicated as setting 0 to 16 in the figures. At different settings, we have different gains and distortion

Table 1
Optimal value of M and optimal positive gains A_m with their multiplicity for a 1 dB difference from the 3 dB slope line.

K	M	A_m	Multiplicy
1, 2	1	1.0000	1
3, 4	3	0.5459	2
		1.0000	1
5, 6	5	0.3411	3
		0.8491	1
		1.0000	1
7, 8	7	0.2470	4
		0.6670	1
		0.9235	1
		1.0000	1
9, 10	9	0.1922	5
		0.5419	1
		0.7989	1
		0.9523	1
		1.0000	1

Table 2
Optimal value of M and optimal positive gains A_m with their multiplicity for a 0.5 dB difference from the 3 dB slope line.

K	M	A_m	Multiplicy
1, 2	1	1.0000	1
3, 4	4	0.5351	3
		1.0000	1
5, 6	6	0.3320	4
		0.8421	1
		1.0000	1
7, 8	9	0.2366	6
		0.6560	1
		0.9226	1
		1.0000	1
9, 10	12	0.1823	8
		0.5307	1
		0.7971	1
		0.9518	1
		1.0000	1

Table 3
$\hat{A}$ for the values of K and M reported in Tables 1 and 2.

K	M	$\frac{\text{MSD}_{\text{PMV}}}{\sigma_v^2}$	$\hat{A}$
1, 2	1	0.5	1
3, 4	3	1.79	0.30
3, 4	4	1.22	0.32
5, 6	5	3.00	0.18
5, 6	6	2.34	0.19
7, 8	7	4.26	0.13
7, 8	9	3.03	0.14
9, 10	9	5.58	0.10
9, 10	12	3.78	0.11

levels. Figure 4 shows the second, third, and total harmonic distortions at different settings on a sinusoidal signal having the same power as the test signals with the highest power considered in the experiments.

Different test signals were applied to the preamplifier, and the corresponding outputs were recorded at a 44 100 Hz sampling frequency. Specifically, the test signals are

- a MLS with period 16,383,
- an ODD-PSEQ with semi-period 16,382,
- an exponential sweep (ES) with length 16,384.
- an OPS input sequence with period 2,097,152.

The ODD-PSEQs are sequences with perfect autocorrelation (a pulse train), whose period is composed of two semi-periods, one the opposite of the other. They are particularly suited to the PMV method because each period allows one to obtain two measures with opposite gains. The exponential sweep was generated as in

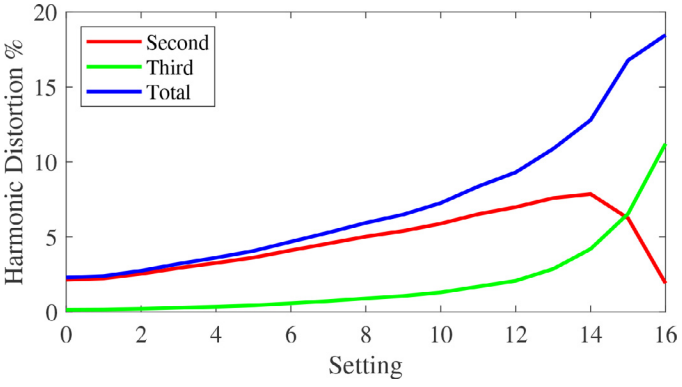

Fig. 4. Second, third, and total harmonic distortion of the MIC100 preamplifier at the different settings.

Novak et al. [41], and sweeps between 18.79 Hz and 20,218 Hz. The initial and final frequencies have been optimized to obtain a sequence that starts and ends with a zero sample.

The OPS input sequence, which has samples with a Gaussian distribution, is used to obtain a good reference for the measured impulse response to compare the different methods. It has longer period than the other sequences and was played with a power 20 dB lower than the maximum power used for the other test signals. For this input, an OPS suitable for identifying the first-order kernel of a Volterra filter of order 3, memory length 128, and diagonal number 5 was developed according to Carini et al. [50] and was used to estimate the reference impulse response for the system under test. Protection until the third order, combined with the low power of the input sequence, confers strong immunity against nonlinearities to the OPS. Its long period also guarantees robustness against noise, resulting in a good reference for other test signals.

MLS, ODD-PSEQ, and ES were applied multiple times with different gains, considering the same power for the different sequences. In particular, the gains in Table 2 for orders $K = 2$, 4, and 6 were considered to perform identification using the PMV method. To allow comparison of the same amount of data, for each gain, 12 repetitions of the periodic or sweep sequence were recorded. The impulse response was identified for each of the 12 recorded sequences. As shown in Appendix A, with MLSs and ODD-PSEQs, identification is based on cross-correlation, and with ESs, it is based on deconvolution. The measurements were then used for PMV identification with orders $K = 2$, 4, and 6. According to Table 2, they require 2, 8, and 12 measurements, respectively, with different gains. Furthermore, to allow comparison of the same amount of data we have also averaged the identifications with the classical methods at the same gain over 2, 8, and 12 measurements.

The recorded signals had high SNR of approximately 70 dB at the maximum gain (gain 1) and 60 dB at the lowest gain (gain 0.332). The different methods were first compared under these high-SNR conditions. Later, white Gaussian noise was added to the output signals to study the effect of low-SNR conditions.

Fig. 5 shows the identification results obtained at the different settings in the high SNR conditions. The results are given in terms of the log spectral distance (LSD) in the band $[100, 18, 000]$ Hz, falling strictly inside the passband of the measurement system. Considering $|H(k)|$ as the measured magnitude response using an FFT on T samples and $|H_{\text{Ref}}(k)|$ as the reference magnitude response obtained with the OPS, the LSD is defined in the band $B = [k_1 \frac{F_S}{T}, k_2 \frac{F_S}{T}]$, with k_1 and $k_2 \in \mathbb{N}$, as follows:

$$\text{LSD} = \sqrt{\frac{1}{k_2 - k_1 + 1} \sum_{k=k_1}^{k_2} \left[10 \log_{10} \frac{|H_{\text{Ref}}(k)|^2}{|H(k)|^2} \right]^2}. \tag{30}$$

In Fig. 5, the bold black curve refers to the results of the PMV method, and the thin curves refer to the results obtained by averaging the multiple measures with the classical methods. The plots in the first row refer to the MLS identification method, those in the second row refer to the ODD-PSEQ identification, and those in the third row refer to the exponential sweeps. In each plot, together with the results of the PMV method, we present the results obtained with the corresponding linear method averaged on the same number of measurements and using the same gains of PMV identification. In the first column, we have the results for PMV order 2. In this case, all the curves coincide, indicating that under the considered conditions, all methods are insensitive to second-order distortion. In fact, the curve of the LSD exhibits very similar behavior to the third-order distortion in Fig. 4. The second and third columns provide the results for PMV orders 4 and 6, respectively.

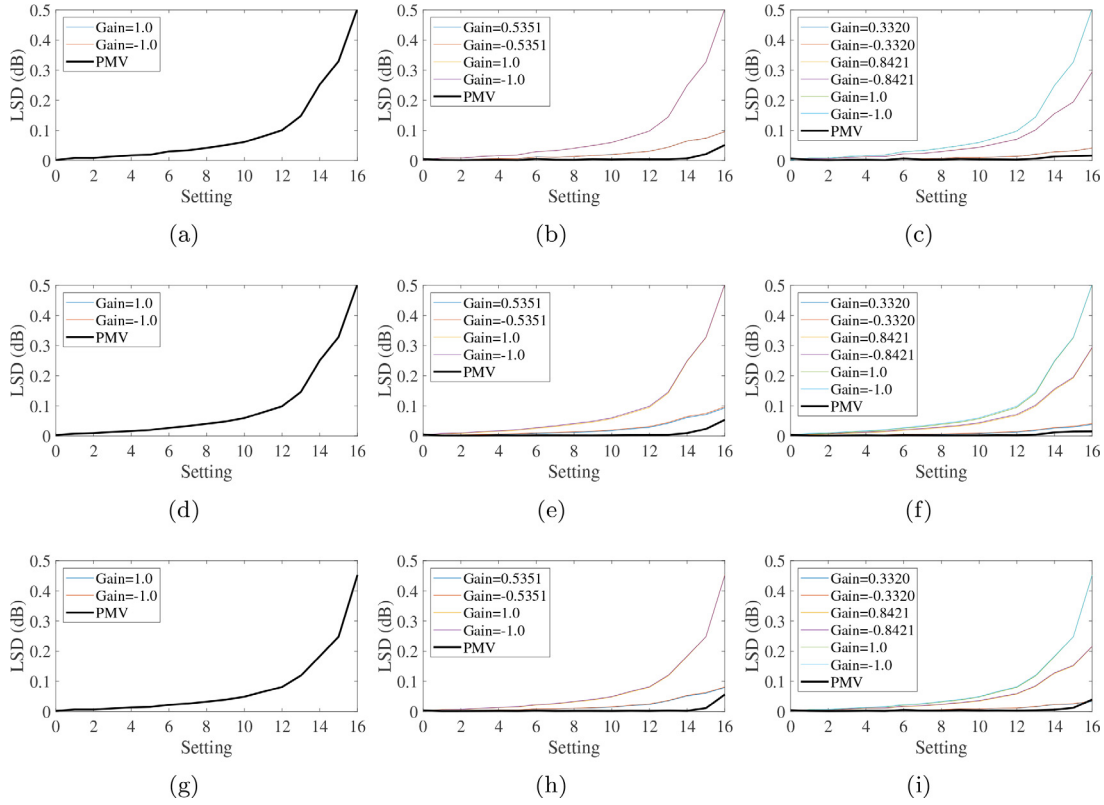

Fig. 5. Log spectra distance in dB at different settings for the proposed method (thick black line) and for multiple averages at the same gains and on the same amount of data, with MLSs ((a), (b), (c)), ODD-PSEQs ((d), (e), (f)), ESs ((g), (h), (i)), for PMV order 2 ((a), (d), (g)), 4 ((b), (e), (h)), 6 ((c), (f), (i)).

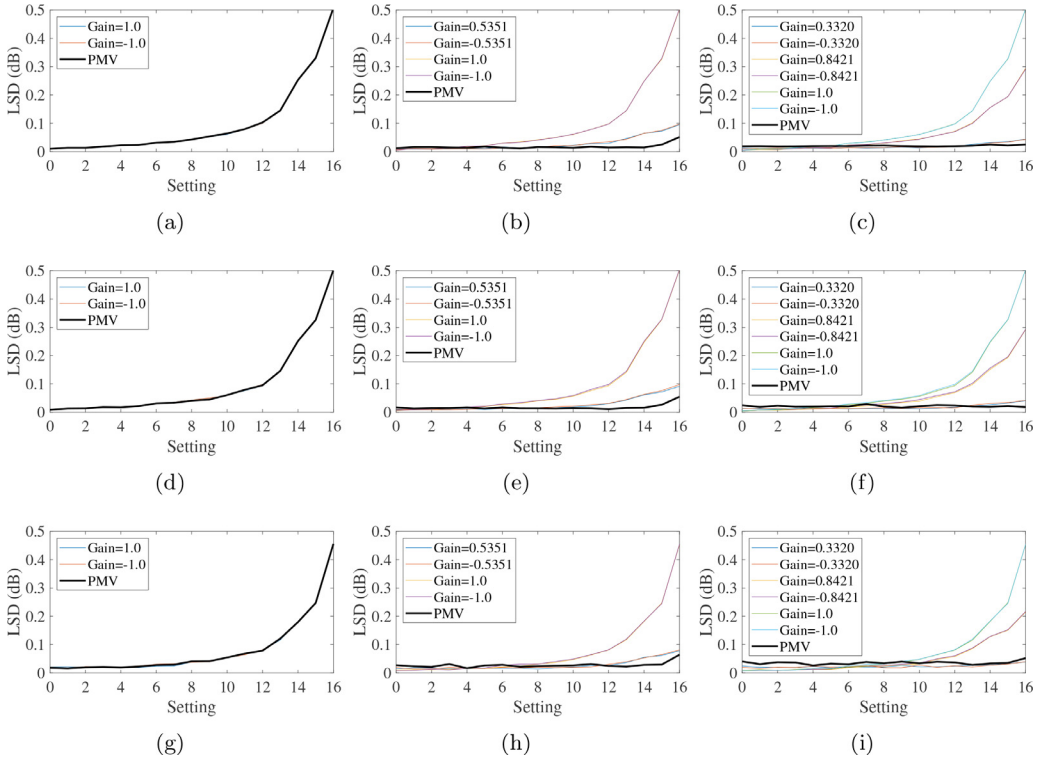

Fig. 6. Log spectra distance in dB at the different settings for the proposed method (thick black line) and for multiple averages at same gains and on the same amount of data for a 20 dB SNR, with MLSs ((a), (b), (c)), ODD-PSEQs ((d), (e), (f)), ESs ((g), (h), (i)), for PMV order 2 ((a), (d), (g)), 4 ((b), (e), (h)), 6 ((c), (f), (i)).

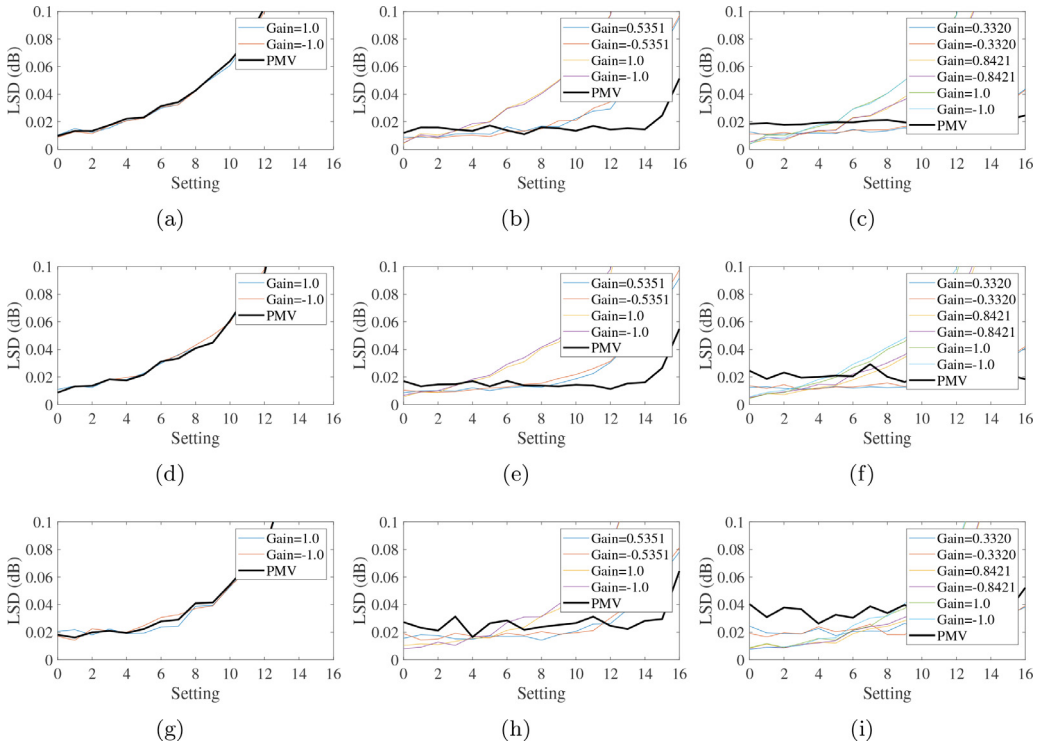

Fig. 7. Detailed plot of log spectra distance in dB at the different settings for the proposed method (thick black line) and for multiple averages at same gains and on the same amount of data for a 20 dB SNR, with MLSs ((a), (b), (c)), ODD-PSEQs ((d), (e), (f)), ESs ((g), (h), (i)), for PMV order 2 ((a), (d), (g)), 4 ((b), (e), (h)), 6 ((c), (f), (i)).

The PMV curves are very flat; only for the last settings, a slight increment is observed, caused by higher-order distortions introduced by the power amplifier. PMV order 4 is sufficient for modeling the power amplifier until setting 14, and only with settings 15 and 16 a slight improvement is obtained using PMV order 6. In the second and third columns, the PMV curves always show better or similar results than the thin curves obtained with multiple averaged measurements. Only at the smallest setting in the measurements with exponential sweeps, the PVM of order 6 shows slightly worse results than the thin curves. This behavior is due to the higher sensitivity of the exponential sweep measurement to noise, as discussed later when the effect of noise is studied.

In this experiment, the measurements with MLSs and ODD-PSEQs were equally sensitive to third-order nonlinearities. In contrast, even though they are also affected, exponential sweeps provide a more robust measurement because the thin LSD curves at the highest settings are always lower than those of the other methods. Nevertheless, the proposed PMV method can be used to extract a more accurate estimate of the impulse response.

To study the effect of noise, we added to all recorded signals (apart from the reference OPS) a white Gaussian noise with zero mean and a certain variance, the same for all signals. The same noise variance was used for all test signals because this is the condition we have in a real measurement. The SNR clearly changes with the gain used for a particular sequence. In the following, the SNR of the maximum gain sequence is used as a reference, and the SNR for the lowest gain sequence (gain 0.332) is 10 dB lower. For each noise variance, we considered 200 different realizations of the noise to allow ensemble measurement of the LSD. For an SNR of the maximum gain sequence equal to or higher than 40 dB, we do not observe any difference from the curves in Fig. 5. On the contrary, for lower SNRs, some differences start to appear. Figure 6 shows the ensemble average of the LSDs at the different settings for a 20 dB SNR and Fig. 7 shows the same information with an enlarged vertical scale. The plots are organized as in Fig. 5.

The estimation with a PMV order $K = 2$ is robust towards the noise and the curves are practically identical to those of Fig. 5. With PMV order $K = 4$ and particularly with $K = 6$ we can observe the effect of noise on the PMV measurement. At the highest settings and distortions, the PMV measurement is still convenient with respect to the classical measurements. Anyway, the curve of LSD has raised and at the lowest settings, it provides an LSD higher than the classical methods. This observation is in agreement with the theory presented in Section 5. The nonlinear terms are considered negligible when their effect is masked by the noise. The higher the noise, the higher the input power for which the nonlinearities are negligible. In Fig. 5, at almost all settings condition (29) is satisfied, and in Figs. 6 and 7, this is not the case for the lowest settings, where the PMV curves are higher than the thin curves. The method that is most affected by noise is based on the exponential sweep, which is also the most robust method against nonlinearities, as noted earlier.

7. Conclusion

We presented a method for measuring the first-order Volterra kernel, that is, the impulse response for low signal amplitudes of nonlinear systems. This approach is based on the use of classical linear identification methods, but the excitation is now applied multiple times using different gains, and the impulse response is estimated with a polynomial interpolation of various measures. We derived the expression of the MSD of the impulse response samples for an additive Gaussian noise and used it to derive the optimal values of the gains and optimal number of measurements. We showed that the optimal gains assume a reduced number of values that depend on the order of nonlinearity of the system. Moreover, we discussed when the proposed method is advantageous compared to classical linear methods applied with low input powers to avoid nonlinearities. The proposed approach is often advantageous even for very mild nonlinear systems. The experimental re-

sults highlight the strengths of the proposed approach and its easy applicability using linear instruments commonly used for impulse-response measurements.

Declaration of Competing Interest

The authors declare that they have no known competing financial interests or personal relationships that could have appeared to influence the work reported in this paper.

CRediT authorship contribution statement

Alberto Carini: Conceptualization, Data curation, Formal analysis, Funding acquisition, Investigation, Methodology, Project administration, Resources, Software, Supervision, Validation, Visualization, Writing – original draft, Writing – review & editing. **Riccardo Forti:** Conceptualization, Data curation, Formal analysis, Investigation, Methodology, Software, Validation, Writing – review & editing. **Simone Orcioni:** Conceptualization, Formal analysis, Methodology, Supervision, Validation, Writing – review & editing.

Data availability

Data will be made available on request.

Appendix A. Examples of linear operator $\mathcal{L}_i$

An example of the linear operator $\mathcal{L}_i$ in (10) is the cross-correlation operator used for impulse response estimation with MLSs and perfect periodic sequences (PPSs):

$$\mathcal{L}_i[y] = \frac{< x(n)y(n) >_L}{< x^2(n) >_L}, \tag{A.1}$$

where $< \cdot >_L$ indicates the sum of L consecutive samples of the term within angular brackets, and L is the MLS or PPS period.

Another example is the deconvolution operator used for impulse response estimation with exponential sweeps,

$$\mathcal{L}_i[y] = \mathrm{IFFT}_i[(\mathrm{FFT}(y) .* \mathrm{FFT}^*(x)) ./ (\mathrm{FFT}(x) .* \mathrm{FFT}^*(x) + \delta)], \tag{A.2}$$

where IFFT_i is the ith sample of the inverse fast Fourier transform, FFT is the fast Fourier transform, $.*$ and $./$ are the sample-by-sample product and division, respectively, and δ is a small positive constant.

For the measurement with OPS, the operator $\mathcal{L}_i$ is the following,

$$\mathcal{L}_i[y] = < z(n)y(n) >_L \tag{A.3}$$

where $z(n)$ is the OPS sequence, and L is its period.

Appendix B. MSD on multiple averaged low amplitude measurements

Let us assume in (9) that we can neglect the constant term for $k = 0$ (e.g., because we have compensated it). Considering $\mathcal{L}_i\mathcal{H}_0 = 0$ and $A_m = A$ for all m, we obtain the following from (13):

$$\mathcal{L}_i(y_m) = A\mathcal{L}_i\mathcal{H}_1(x) + \sum_{k=2}^{K} A^k \mathcal{L}_i\mathcal{H}_k(x) + \mathcal{L}_i(v_m), \tag{B.1}$$

We perform $2M$ measurements and estimate $h_{1,i} = \mathcal{L}_i\mathcal{H}_1(x)$ with

$$\widehat{h}_{1,i} = \frac{\sum_{m=1}^{2M} \mathcal{L}_i(y_m)}{2MA} = h_{1,i} + \sum_{k=2}^{K} A^{k-1}\mathcal{L}_i\mathcal{H}_k(x) + \frac{\sum_{m=1}^{2M} \mathcal{L}_i(v_m)}{2MA}. \tag{B.2}$$

Note that the nonlinear terms in (B.2) reduce at least linearly with A. Thus, for sufficiently low A the nonlinear terms can be neglected, and

$$\widehat{h}_{1,i} = h_{1,i} + \frac{\sum_{m=1}^{2M} \mathcal{L}_i(v_m)}{2MA}. \tag{B.3}$$

In the hypothesis that the noise terms $\mathcal{L}_i(v_m)$ are uncorrelated with each other, Gaussian distributed with zero mean and variance σ_v^2, the MSD is

$$\mathrm{MSD}_{\mathrm{Av}} = E[(h_{1,i} - \widehat{h}_{1,i})^2] = \frac{\sigma_v^2}{2MA^2}. \tag{B.4}$$

References

[1] R. Maruyama, N. Kuwaki, S. Matsuo, M. Ohashi, Relationship between mode coupling and fiber characteristics in few-mode fibers analyzed using impulse response measurements technique, J. Lightwave Technol. 35 (4) (2016) 650–657.
[2] J.-H. Hwang, T.-W. Kang, Y.-T. Kim, S.-O. Park, Measurement of transmission properties of HBC channel and its impulse response model, IEEE Trans. Instrum. Meas. 65 (1) (2015) 177–188.
[3] Y. Fujii, Measurement of impulse response of force transducers, Rev. Sci. Instrum. 72 (7) (2001) 3108–3111.
[4] A. Ledergerber, M. Hamer, R. D'Andrea, Angle of arrival estimation based on channel impulse response measurements, in: 2019 IEEE/RSJ International Conference on Intelligent Robots and Systems (IROS), IEEE, 2019, pp. 6686–6692.
[5] M. Nathan, T.S. Keller, Measurement and analysis of the in vivo posteroanterior impulse response of the human thoracolumbar spine: a feasibility study, J. Manip. Physiol. Ther. 17 (7) (1994) 431–441.
[6] B. Zhou, D.M. Green, J.C. Middlebrooks, Characterization of external ear impulse responses using Golay codes, J. Acoust. Soc. Am. 92 (2) (1992) 1169–1171.
[7] D. Auston, Impulse response of photoconductors in transmission lines, IEEE J. Quantum Electron. 19 (4) (1983) 639–648.
[8] P. Smith, D. Auston, W. Augustyniak, Measurement of GaAs field-effect transistor electronic impulse response by picosecond optical electronics, Appl. Phys. Lett. 39 (9) (1981) 739–741.
[9] H. Hashemi, Impulse response modeling of indoor radio propagation channels, IEEE J. Sel. Areas Commun. 11 (7) (1993) 967–978.
[10] M. Mazur, N.K. Fontaine, R. Ryf, H. Chen, A. Blanco-Redondo, Impulse response measurement of a few-mode fiber using superconducting nanowire single-photon detectors, in: 2021 European Conference on Optical Communication (ECOC), IEEE, 2021, pp. 1–4.
[11] Z. Petojević, R. Gospavić, G. Todorović, Estimation of thermal impulse response of a multi-layer building wall through in-situ experimental measurements in a dynamic regime with applications, Appl. Energy 228 (2018) 468–486.
[12] K. Kanokkanchana, E.N. Saw, K. Tschulik, Nano impact electrochemistry: effects of electronic filtering on peak height, duration and area, ChemElectroChem 5 (20) (2018) 3000–3005.
[13] R. Barnichon, C. Matthes, Functional approximation of impulse responses, J. Monet. Econ. 99 (2018) 41–55.
[14] Y. Ding, Z. Cheng, X. Zhu, K. Yvind, J. Dong, M. Galili, H. Hu, N.A. Mortensen, S. Xiao, L.K. Oxenløwe, Ultra-compact integrated graphene plasmonic photodetector with bandwidth above 110 GHz, Nanophotonics 9 (2) (2020) 317–325.
[15] W. Klippel, Tutorial: loudspeaker nonlinearities-causes, parameters, symptoms, J. Audio Eng. Soc. 54 (10) (2006) 907–939.
[16] M. Schetzen, The Volterra and Wiener Theories of Nonlinear Systems, Wiley, 1980.
[17] V.J. Mathews, G.L. Sicuranza, Polynomial Signal Processing, Wiley, New York, NY, 2000.
[18] J.M. Berman, L.R. Fincham, The application of digital techniques to the measurement of loudspeakers, J. Audio Eng. Soc. 25 (6) (1977) 370–384.
[19] M.R. Schroeder, Integrated-impulse method measuring sound decay without using impulses, J. Acoust. Soc. Am. 66 (2) (1979) 497–500.
[20] C. Dunn, M. Hawksford, Distortion immunity of MLS-derived impulse response measurements, J. Audio Eng. Soc. 41 (5) (1993) 314–335.
[21] C. Antweiler, M. Dörbecker, Perfect sequence excitation of the NLMS algorithm and its application to acoustic echo control, Ann. Telecommun. 49 (7–8) (1994) 386–397.
[22] H. Luke, H. Schotten, Odd-perfect, almost binary correlation sequences, IEEE Trans. Aerosp. Electron. Syst. 31 (1) (1995) 495–498.
[23] N. Aoshima, Computer-generated pulse signal applied for sound measurement, J. Acoust. Soc. Am. 69 (5) (1981) 1484–1488.
[24] Y. Suzuki, F. Asano, H.Y. Kim, T. Sone, An optimum computer-generated pulse signal suitable for the measurement of very long impulse responses, J. Acoust. Soc. Am. 97 (2) (1995) 1119–1123.
[25] S. Foster, Impulse response measurement using Golay codes, in: ICASSP'86. IEEE International Conference on Acoustics, Speech, and Signal Processing, vol. 11, IEEE, 1986, pp. 929–932.
[26] R.C. Heyser, Acoustical measurements by time delay spectrometry, J. Audio Eng. Soc. 15 (1967) 370–382.
[27] H. Biering, O.Z. Pedersen, System analysis and time delay spectrometry (part I), Brüel Kjær Tech. Rev. (1) (1983) 3–51.

[28] J. Schoukens, R.M. Pintelon, Y.J. Rolain, Broadband versus stepped sine FRF measurements, IEEE Trans. Instrum. Meas. 49 (2) (2000) 275–278, doi:10.1109/19.843063.
[29] C. Antweiler, A. Telle, P. Vary, G. Enzner, Perfect-sweep NLMS for time-variant acoustic system identification, in: Proc. of ICASSP 2012, 2012, pp. 517–520.
[30] F.J. MacWilliams, N.J. Sloane, Pseudo-random sequences and arrays, Proc. IEEE 64 (12) (1976) 1715–1729.
[31] J. Vanderkooy, Aspects of MLS measuring systems, J. Audio Eng. Soc. 42 (4) (1994) 219–231.
[32] M. Wright, J. Vanderkooy, Comments on -aspects of MLS measuring systems- and author's reply, J. Audio Eng. Soc. 43 (1/2) (1995) 48,49.
[33] R. Ream, Nonlinear identification using inverse-repeat m sequences, Proc. IEE (London) 117 (1970) 213–218.
[34] C. Antweiler, M. Antweiler, System identification with perfect sequences based on the NLMS algorithm, AEU-Arch. Elektron. Ubertrag. 49 (3) (1995) 129–134.
[35] C. Antweiler, Multi-Channel System Identification with Perfect Sequences-Theory and Applications-, John Wiley & Sons, Ltd, 2008, pp. 171–198.
[36] V. Ipatov, Ternary sequences with ideal periodic autocorrelation properties, Radio Eng. Electron. Phys. 24 (1979) 75–79.
[37] H.D. Luke, Sequences and arrays with perfect periodic correlation, IEEE Trans. Aerosp. Electron. Syst. 24 (3) (1988) 287–294.
[38] M.F. Antweiler, L. Bomer, H.-D. Luke, Perfect ternary arrays, IEEE Trans. Inf. Theory 36 (3) (1990) 696–705.
[39] A. Farina, Simultaneous measurement of impulse response and distortion with a swept-sine technique, Audio Engineering Society Convention 108, Paris, France, 2000.
[40] S. Müller, P. Massarani, Transfer-function measurement with sweeps, J. Audio Eng. Soc. 49 (6) (2001) 443–471.
[41] A. Novak, P. Lotton, L. Simon, Synchronized swept-sine: theory, application, and implementation, J. Audio Eng. Soc. 63 (10) (2015) 786–798.
[42] T. Schmitz, J.-J. Embrechts, Hammerstein kernels identification by means of a sine sweep technique applied to nonlinear audio devices emulation, J. Audio Eng. Soc. 65 (9) (2017) 696–710.
[43] A. Torras-Rosell, F. Jacobsen, A new interpretation of distortion artifacts in sweep measurements, J. Audio Eng. Soc. 59 (5) (2011) 283–289.
[44] D.G. Ćirić, M. Marković, M. Mijić, D. Šumarac Pavlović, On the effects of nonlinearities in room impulse response measurements with exponential sweeps, Appl. Acoust. 74 (3) (2013) 375–382.
[45] A. Carini, S. Cecchi, L. Romoli, Room impulse response estimation using perfect sequences for Legendre nonlinear filters, in: 2015 23rd European Signal Processing Conference (EUSIPCO), 2015, pp. 2541–2545.
[46] A. Carini, S. Cecchi, L. Romoli, Robust room impulse response measurement using perfect sequences for Legendre nonlinear filters, IEEE/ACM Trans. Audio, Speech, Lang. Process. 24 (11) (2016) 1969–1982.
[47] A. Carini, S. Cecchi, A. Terenzi, S. Orcioni, On room impulse response measurement using perfect sequences for Wiener nonlinear filters, in: 2018 26th European Signal Processing Conference (EUSIPCO), 2018, pp. 982–986.
[48] A. Carini, S. Cecchi, S. Orcioni, Robust room impulse response measurement using perfect periodic sequences for Wiener nonlinear filters, Electronics 9 (11) (2020).
[49] A. Carini, G.L. Sicuranza, Perfect periodic sequences for even mirror Fourier nonlinear filters, Signal Process. 104 (2014) 80–93.
[50] A. Carini, S. Orcioni, A. Terenzi, S. Cecchi, Orthogonal periodic sequences for the identification of functional link polynomial filters, IEEE Trans. Signal Process. 68 (2020) 5308–5321.
[51] A. Carini, S. Orcioni, S. Cecchi, On room impulse response measurement using orthogonal periodic sequences, in: 2019 27th European Signal Processing Conference (EUSIPCO), 2019, pp. 1–5.
[52] A. Carini, S. Cecchi, A. Terenzi, S. Orcioni, A room impulse response measurement method robust towards nonlinearities based on orthogonal periodic sequences, IEEE/ACM Trans. Audio, Speech, Lang. Process. 29 (2021) 3104–3117.
[53] R. Forti, A. Carini, S. Orcioni, Polynomial multiple variance impulse response measurement, IWAENC 2022. International Workshop on Acoustic Signal Enhancement, IEEE, 2022.
[54] S. Orcioni, Improving the approximation ability of Volterra series identified with a cross-correlation method, Nonlinear Dyn. 78 (4) (2014) 2861–2869.
[55] S. Orcioni, A. Terenzi, S. Cecchi, F. Piazza, A. Carini, Identification of Volterra models of tube audio devices using multiple-variance method, J. Audio Eng. Soc. 66 (10) (2018) 823–838.
[56] T. Roinila, T. Messo, Online grid-impedance measurement using ternary-sequence injection, IEEE Trans. Ind. Appl. 54 (5) (2018) 5097–5103.
[57] S. Kannan, J. Meyer, Recent developments in harmonic resonance detection in low voltage networks using impedance measurement techniques, in: 2019 8th International Conference on Power Systems (ICPS), IEEE, 2019, pp. 1–6.
[58] E. Von Hauff, Impedance spectroscopy for emerging photovoltaics, J. Phys. Chem. C 123 (18) (2019) 11329–11346.
[59] F. Ciucci, Modeling electrochemical impedance spectroscopy, Curr. Opin. Electrochem. 13 (2019) 132–139.
[60] A. Altan, R. Hacıoğlu, Model predictive control of three-axis gimbal system mounted on UAV for real-time target tracking under external disturbances, Mech. Syst. Signal Process. 138 (2020) 106548.
[61] S. Tamilselvi, S. Gunasundari, N. Karuppiah, A. Razak RK, S. Madhusudan, V.M. Nagarajan, T. Sathish, M.Z.M. Shamim, C.A. Saleel, A. Afzal, A review on battery modelling techniques, Sustainability 13 (18) (2021) 10042.
[62] N. Meddings, M. Heinrich, F. Overney, J.-S. Lee, V. Ruiz, E. Napolitano, S. Seitz, G. Hinds, R. Raccichini, M. Gaberšček, et al., Application of electrochemical impedance spectroscopy to commercial Li-ion cells: a review, J. Power Sources 480 (2020) 228742.
[63] O. Gharbi, M.T. Tran, B. Tribollet, M. Turmine, V. Vivier, Revisiting cyclic voltammetry and electrochemical impedance spectroscopy analysis for capacitance measurements, Electrochim. Acta 343 (2020) 136109.
[64] Y. Chen, L. Yang, L. Zhou, X. Jin, G. Jia, Calibration of hydrophones using a frequency domain filter processing method: theory and experiment, Meas. Sci. Technol. 32 (3) (2020) 035012.
[65] W. Gautschi, Optimally conditioned vandermonde matrices, Numer. Math. 24 (1) (1975) 1–12.
[66] W. Gautschi, Optimally scaled and optimally conditioned vandermonde and vandermonde-like matrices, BIT Numer. Math. 51 (1) (2011) 103–125.